Activation of 3-Hydroxypropionate by Addition of Coenzyme A by *Rhodobacter sphaeroides*

Research Thesis

Presented in partial fulfillment of the requirements for graduation *with research distinction* in Microbiology in the College of Arts and Sciences of The Ohio State University

by

Sydney P. Alibeckoff

The Ohio State University

November 2018

Project Advisor: Dr. Birgit E. Alber, Department of Microbiology

Abstract

The metabolically diverse bacterium, *Rhodobacter sphaeroides*, was employed to study the assimilation of 3-hydroxypropionate during photoheterotrophic growth, specifically to test the hypothesis that 3-hydroxypropionate is activated via addition of a coenzyme A (CoA) thiol. One class of enzymes postulated to be responsible for catalyzing this reaction is AMP-forming synthetases, which hydrolyze ATP to add a free CoA to the target molecule. Several genes, *rsp_0579* (*acs*) and *rsp_1592* (*pcst*), with the potential to encode a 3-hydroxypropionyl-CoA synthetase were bioinformatically identified in the genome of *R. sphaeroides*. The purpose of this study was to characterize an annotated propionyl-CoA synthetase (Pcst) using a genetic and biochemical approach in order to determine its role in 3-hydroxypropionate assimilation. An in-frame *pcst* deletion mutant of *R. sphaeroides* (Δpcst) was generated; increased doubling time of Δpcst was observed during growth with 3-hydroxy propionate as the sole carbon source. Additionally, a decrease in CoA synthetase-specific activity towards acetate, propionate, and 3-hydroxypropionate was detected in the cell extract of Δpcst. A CoA synthetase-specific substrate dependence assays of heterologously produced and purified His_6-tagged Pcst show a 100-fold higher catalytic efficiency of Pcst with propionate in comparison to acetate and 3-hydroxy-propionate. Pcst was characterized as a propionyl-CoA synthetase that displayed lower activity with substrates acetate and 3-hydroxypropionate. Pcst appears to contribute to assimilation of 3-hydroxypropionate *in vivo*, although not as the sole enzyme.

Table of Contents

Introduction

3-Hydroxypropionate serves as an important chemical in industry for the synthesis of products such as acrylate and 3-hydroxypropionate-based polymers[1,2]. Therefore, attention has been given to metabolic engineering of bacteria for the production and isolation of 3-hydroxypropionate. However, 3-hydroxypropionate can be used by bacteria as both an intermediate in carbon metabolism[3] and as a sole carbon source[4], which can lower the yield of 3-hydroxypropionate production in engineered strains. Understanding the mechanisms by which 3-hydroxypropionate is assimilated can assist in construction of strains that are unable to use this compound as a carbon substrate, thereby increasing 3-hydroxypropionate production in these organisms.

The model organism utilized to study 3-hydroxypropionate assimilation is *Rhodobacter sphaeroides*, which is an anoxygenic photoheterotrophic bacterium characterized as being metabolically diverse due to its ability to grow with a variety of carbon substrates. When grown photoheterotrophically, 3-hydroxypropionate is used exclusively as a carbon source rather than an energy source, allowing the study of its assimilation. The known routes of 3-hydroxypropionate assimilation are oxidation to produce acetyl-CoA, and reduction to produce

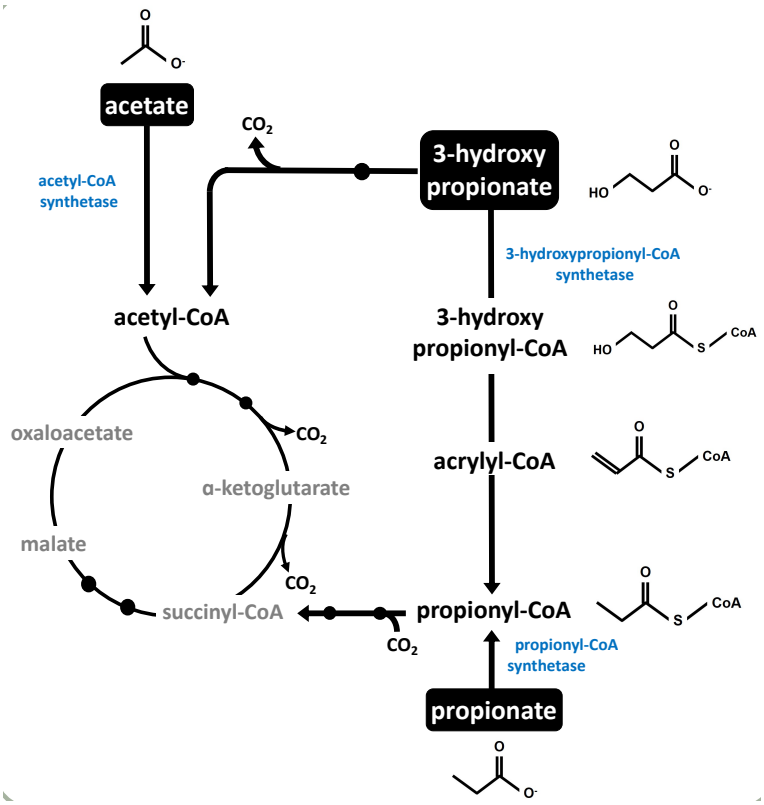

Figure 1. Hypothesized model for reductive assimilation of 3-hydroxypropionate. The focus is on carbon flow and no cofactors are included.

propionyl-CoA with subsequent addition of CO_2 to form succinyl-CoA (Fig. 1). Evidence for reductive assimilation of 3-hydroxypropionate comes from the necessity of acrylyl-coenzyme A reductase and formation of 3-hydroxypropionyl-CoA when 3-hydroxypropionate, ATP, and CoA were added to cell extracts of *R. sphaeroides*[4]. The presence of 3-hydroxypropionyl-CoA upon addition of 3-hydroxypropionate suggests that activation of 3-hydroxypropionate is required prior to dehydration to acrylyl-CoA. Addition of coenzyme A (CoA) may be necessary due to the ability of CoA to act as an electron withdrawing group, which facilitates the dehydration of 3-hydroxypropionate-CoA to acrylyl-CoA. While the addition of CoA to 3-hydroxypropionate is a likely step in the reductive assimilation of 3-hydroxypropionate, the enzyme that catalyzes this reaction has not been identified.

Several classes of enzymes have been identified with the potential to catalyze this reaction, including CoA transferases[5], kinases/transacetylases[6], and CoA synthetases[7]. One class of enzymes hypothesized to be responsible for catalyzing this reaction is an AMP-forming acyl-CoA synthetase, which hydrolyze ATP to add a free CoA to the target molecule. This class of enzymes has the potential to exhibit activity with multiple carbon substrates *in vivo*; a highly-

specific propionyl-CoA synthetase found in *Salmonella enterica* has the ability replace the function of an acetyl-CoA synthetase despite having low substrate specificity to acetate[7]. This suggests that synthetases found in *R. sphaeroides* may have the ability to function with 3-hydroxypropionate, even if the synthetase has low specificity with 3-hydroxypropionate.

Two synthetase genes were bioinformatically identified in the genome of *R. sphaeroides*; *rsp_0579*, which is annotated as encoding an acetyl-CoA synthetase (*acs*), and *rsp_1592*, which is annotated as encoding a propionyl-CoA synthetase (*pcst*). These genes were annotated based on amino acid residue similarity to previously characterized acyl-CoA synthetases. Rsp_0579 displayed 49% amino acid sequence identity to an acetyl-CoA synthetase found in *Mycobacterium tuberculosis* with high specificity with acetate and propionate[8], and Rsp_1592 displayed 44% amino acid identity with the propionyl-CoA synthetase (PrpE) studied in *S. enterica*[7], suggesting that the synthetases found in *R. sphaeroides* may be similar in function and substrate specificity to the homologous synthetases found in other organisms. Additionally, unpublished work performed in the Alber Laboratory has shown Acs from *R. sphaeroides* to have substrate specificity with acetate and propionate. However, Pcst has not been previously studied and characterized in *R. sphaeroides*. An acetyl- or propionyl-CoA synthetase is hypothesized to have the ability to catalyze the addition of CoA to 3-hydroxypropionate due to the molecular similarity of 3-hydroxypropionate to acetate and propionate; all are short chain fatty acids that only differ in carbon number and a single functional group.

This study focuses on analysis of the role of the Pcst found in *R. sphaeroides* both *in vivo* and *in vitro*, and its potential to assist in the assimilation of 3-hydroxypropionate. Characterization of the role of Pcst *in vivo* was determined by quantifying growth of *pcst* deletion mutants with 3-hydroxypropionate as the sole carbon source, as well as detection of CoA synthetase-specific activity of *R. sphaeroides* cell extracts with either the presence or

absence of *pcst* in its genome. Characterization of Pcst *in vitro* included detection of CoA synthetase-specific activity of heterologously produced and purified Pcst to determine kinetic parameters and substrate specificity.

Methods

Contributions to this work: The construction of pSC75, pSC114, and pSC115 was performed by Steven Carlson (Alber Lab), and construction of pMA24-4, pMA18-4, pMA26-1, and pMA26-1 was performed by Dr. Marie Asao (Alber Lab).

Bacterial strains and growth conditions.

The strains used in this study are listed in Appendix, Table 7. *R. sphaeroides* strain 2.4.1 was grown at pH 6.7 and at 30 °C aerobically in the dark or anaerobically in the light (3,000 lx) in defined medium supplemented with 10 mM of the appropriate carbon source[9]. Growth was monitored by determining the optical density at 578 nm (OD578), and cells were harvested in the mid-exponential phase at an OD578 of 0.5 to 0.8. For growth studies, the appropriate *R. sphaeroides* mutant or wild-type was pregrown anaerobically in 3 mL minimal medium containing 10 mM sodium lactate, and 0.1 ml was transferred into stoppered screw-cap (Hungate) tubes with 4 mL minimal medium and the appropriate carbon source. Cells were grown in the presence of 20 μg/mL kanamycin and 25 μg/mL spectinomycin as necessary, which was determined by the antibiotic resistance gene encoded on the plasmid present. *Escherichia coli* strains DH5α, S17-1, and SM10 were grown in Luria-Bertani (LB) broth at 37 °C. For conjugation, *R. sphaeroides* cells were grown aerobically on LB medium in the dark.

Construction of *R. sphaeroides* mutants Δacs, Δpcst, ΔacsΔpcst.

The plasmids and primers used in this study are listed in Appendix, Table 8 and 9, respectively. The suicide plasmid pSC114 employed for the in-frame inactivation of *acs* (*rsp_0579*) was constructed by amplifying 949 bp of an upstream region (primers dASynUp_F and dASynUp_R) and 793 bp of a downstream region (primers dASynDn_F and dASynDn_R) of *acs* by PCR using *R. sphaeroides* genomic DNA as the template. The amplified upstream and downstream regions contained an inserted homologous sequence, which allowed assembly and amplification of the entire deleted region. The assembled PCR product containing the deleted region was ligated into pK18mobsacB using restriction enzymes *Hind*III and *Xba*I. The resulting plasmid, pSC114, contains an in-frame deletion of 1,827 bp of the *acs* gene. The remaining open reading frame includes 105 bp of the 3′ portion of the original coding region and 30 bp of the 5′ portion, encoding a 45-amino-acid peptide.

RsΔacs21SA was isolated by mating *R. sphaeroides* 2.4.1 with *E. coli* S17-1 transformed with pSC114. Single-crossover strains were isolated anaerobically in the light on minimal medium plates containing D/L lactate as the carbon source (minimal medium D/L lactate plates) and kanamycin for selection. Genotyping of the single-crossover strains was performed using primers dASyn_1xo_UpF and dASyn_1xo_UpR to characterize the upstream region, and primers dASyn_1xo_DnF and dASyn_1xo_DnR to characterize the downstream region. The PCR product sizes obtained were used to determine whether an upstream or downstream crossover event occurred. Of the six single-crossover isolates, four were upstream crossovers and two were downstream crossovers. To allow the second crossover event, the cells from isolated colonies were grown aerobically in the dark overnight in 100 µl minimal medium D/L lactate lacking kanamycin. Overnight cultures were spread on minimal medium D/L lactate plates supplemented with 10% (w/v) sucrose and grown anaerobically in the light. Isolated colonies

were patched as replicates on minimal medium D/L lactate plates with or without kanamycin. For identification of double-crossover strains, colony PCR was performed on kanamycin-sensitive strains using primers dASyn_1xo_UpF and dASyn_1xo_DnR. The PCR product sizes obtained were used to distinguish the isolates as deletion mutants or wild-type revertants. The genotype of RsΔacs was confirmed by sequencing the product obtained by PCR with primers dASyn_1xo_DnF and dASyn_1xo_UpR.

A similar strategy was employed to construct the RsΔ*pcst*17SA strain. The plasmid pSC115 utilized for the inactivation of *pcst* (*rsp_0579*) was constructed by amplifying 981 bp of an upstream region (primers dPSynUp_F and dPSynUp_R) and 1019 bp of a downstream region (primers dPSynDn_F and dPSynDn_R of *pcst* by PCR using *R. sphaeroides* genomic DNA as a template, assembling the inactivation product via homologous sequence of the upstream and downstream region, and cloning the product into pK18mobsacB using restriction enzymes *Hind*III and *Xba*I. The resulting plasmid, pSC115, contains an in-frame deletion of 1,749 bp of the *pcst* gene. The remaining open reading frame includes 66 bp of the 3′ portion of the original coding region and 99 bp of the 5′ portion, encoding a 56-amino-acid peptide.

RsΔpcst17SA was isolated by mating *R. sphaeroides* 2.4.1 with *E. coli* S17-1 transformed with pSC115. Single-crossover strains were isolated, and genotyping of the single-crossover strains was performed using primers dPSyn_1xo_UpF and dPSyn_1xo_UpR to characterize the upstream region, and primers dPSyn_1xo_DnF and dPSyn_1xo_DnR to characterize the downstream region. Of the three single-crossover isolates, one was an upstream crossover and two were downstream crossovers. The second crossover event occurred using the same method as RsΔacs21SA. For identification of double-crossover strains, colony PCR was performed on kanamycin-sensitive strains using primers dPSyn_1xo_UpF and dPSyn_1xo_DnR.

The genotype of RsΔpcst17SA was confirmed by sequencing the product obtained by PCR with primers dPSyn_1xo_DnF and dPSyn_1xo_UpR.

The inactivation of both *acs* and *pcst* genes was achieved by performing the same method for the inactivation of *pcst* using RsΔacs21SA as the background strain. RsΔacsΔpcst was isolated by mating RsΔacs21SA with *E. coli* S17-1 transformed with pSC115. After allowing a single crossover event to occur, two upstream and two downstream crossovers were isolated. The second crossover event resulted in three potential ΔacsΔpcst strains; the genotype of RsΔacsΔpcst3SA was confirmed by sequencing the PCR product of the inactivated *pcst* region.

Construction of complementation and expression plasmids.

The expression plasmid pMA27-1 was constructed by amplifying the genetic region containing *pcst* by PCR (primers RSP1592_F4 and RSP1592_R) using *R. sphaeroides* genomic DNA as a template, resulting in a 2155 bp product. The PCR product was ligated into pUC19 (pMA18-4) using restriction enzymes *Nde*I and *Hind*III. Plasmid pMA18-4 was used as a template for amplifying *pcst* due to false priming from *R. sphaeroides* genomic DNA; *pcst* was amplified by PCR (primers RSP1592_NdeIF and RSP1592exp_HindIII), then ligated into pUC19 (pMA26-1) using restriction enzymes *Nde*I and *Hind*III. The *pcst* insert from pMA26-1 was cloned into pET16b (pMA27-1) with *Nde*I and *Hind*III, which resulted in the His_6-tagged gene upstream of *pcst* (N-terminus).

The constitutive *pcst* complementation plasmid (pSA9) was constructed by PCR amplification of *pcst* using pMA27-1 as a template (primers RSP_1592_ndeI_F and acs_speI_R), resulting in a 2062 bp PCR product. The resulting product was ligated into pSC75 (pSA9) using *Nde*I and *Spe*I; pSC75 contains an rrnB promoter, which permits constitutive expression of the gene inserted. pSA9 was confirmed by sequencing the *pcst* region. The native *pcst*

complementation plasmid (pSA11) was constructed by PCR amplification of *pcst* and its native promoter using *R. sphaeroides* genomic DNA as a template (primers pcst_sacI_F and COMPpcst_speI_R), resulting in a 2236 bp PCR product. The resulting product was ligated into pBBR(MC) (pSA11) using *Sac*I and *Spe*I. pSA11 was confirmed by sequencing the pSA11 insert. Complementation plasmids were introduced into *R. sphaeroides* by mating WT and Δpcst with *E. coli* transformed with either pSA9 or pSA11. Spectinomycin was used to select for strains containing the plasmid of interest.

CoA Synthetase Activity Assay.

For the preparation of *R. sphaeroides* cell extracts, 400 to 600 mg frozen cells were resuspended in 0.6 mL 25 mM Tris-HCl (pH 8.0) buffer containing 5 mM $MgCl_2$ and 0.1 mg mL^{-1} DNase I. After the addition of 1 g glass beads (diameter, 0.1 to 0.25 mm), the cell solution was treated in a mixer mill (type MM2; Retsch, Haare, Germany) for 9 min at 30 Hz. Cell debris and glass beads were removed by centrifugation at 14,000 × *g* for 10 min at 4°C. The protein content of the cell extract was estimated to be 2 to 15 mg mL^{-1}. Protein concentrations were determined by Bradford assay, using bovine serum albumin as a standard.

`The AMP-forming addition of CoA to a short-chained fatty acid was monitored by coupling the reaction to NADH oxidation, which was detected spectrophotometrically at 365 nm (ε_{NADH} = 3,400 M^{-1} cm^{-1}) due to historical use of 365 nm to detect NADH oxidation. The enzymes used to couple AMP formation to NADH oxidation were myokinase, pyruvate kinase, and lactate dehydrogenase. The master reaction mixture contained 100 mM Tris-HCl buffer (pH 7.9), 2 mM DTT, 1 mM phosphoenolpyruvate (PEP), 8.6 µg/mL myokinase, 9.7 µg/mL lactate dehydrogenase, and 26.3 µg/mL pyruvate kinase. Since the components within the master mix were determined to be in excess, a variable amount of master mix was added to the reaction to

obtain a final volume of 0.5 mL. Between 427 to 452 µL of master reaction mixture was added with 1.2 mM ATP, 0.6 mM CoA, 0.4 mM NADH, and cell extract containing 0.25 to 1.50 µg protein in a final reaction volume of 0.5 mL. The reaction was initiated at 30 °C using 20 mM acetate, propionate, or 3-hydroxypropionate, and was monitored using a plastic cuvette with a path length of 1.0 cm.

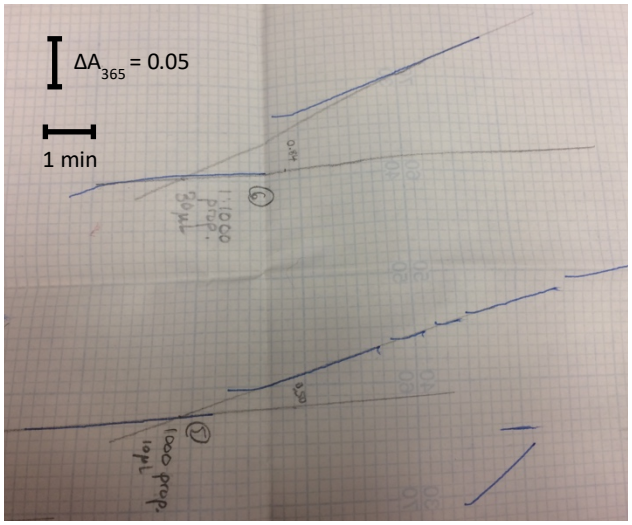

Figure 2. CoA synthetase activity coupled to oxidation of NADH. Distance between background and total change in A_{365} was used to determine net NADH oxidation from synthetase activity.

Change in absorbance at 365 nm was monitored using Kipp and Zonen Flatbed Recorder, recorded at 1.0 cm/min and 1 cm = 0.05 change in absorbance. Background absorbance change was recorded prior to addition of carbon substrate and subtracted from the total absorbance change recorded after addition of carbon substrate (Fig. 2). The distance between the total absorbance rate and background absorbance rate was measured and used to calculate the net change in absorbance per min.

Preparation of cells containing heterologously produced His_6-tagged Pcst.

Expression of the *pcst* gene was achieved by first transforming *E. coli* BL21 (DE-3) with pMA27-1 in the presence of ampicillin. One liter of cells was grown aerobically in LB at 37 °C to an OD578 of 0.6, chilled on ice for 10 min, then induced with 0.4 mM IPTG. Post-induction cells were incubated overnight at 20 °C; 2.0-5.0 g of cells were harvested *via* freezing with liquid N_2.

Purification of His_6-Tagged Pcst.

Frozen *E. coli* cells with heterologous production of His_6-tagged Pcst (H-Pcst) were resuspended in 10 mL Buffer A [25mM Tris-HCl (pH 8.0), 5 mM $MgCl_2$] containing 0.1 mg ml^{-1} DNase I. Lysis of cells was performed *via* French Press, then cell debris and insoluble proteins were removed by ultracentrifugation at 100,000 x g for 1 hr at 4 °C. Ammonium sulfate precipitation was performed by addition of 3.8 M (100%) ammonium sulfate solution at 4 °C to cell extract to achieve 40% ammonium sulfate saturation. H-Pcst was soluble in the supernatant of 40% saturated ammonium sulfate solution as determined by CoA-dependent activity in. The 40% ammonium sulfate supernatant fraction was applied to a Ni-NTA agarose column and the flow-through was collected. Column was washed with Buffer B [20 mM Tris-HCl (pH 7.9), 200 mM KCl] containing 25 mM imidazole, then Buffer B containing 100 mM imidazole to elute weakly binding proteins. H-Pcst was eluted with Buffer B containing 350 mM imidazole; H-Pcst activity was detected in 350 mM imidazole elusion fraction via CoA synthetase enzyme assay. Column was washed with Buffer B containing 500 mM imidazole to ensure removal of H-Pcst. The 350 mM imidazole fraction was dialyzed against Buffer A for three days at 4 °C. The purified protein was stored at -20 °C in 20% (v/v) glycerol and used within two weeks of purification.

Results

Table 1. CoA synthetase-specific activity of *R. sphaeroides* WT, Δpcst, and ΔacsΔpcst cell extracts grown with 3-hydroxypropionate.

CoA Synthetase Specific Activity (nmol/min/mg)[a,b]			
	acetate	propionate	3-hydroxypropionate
WT	270 ± 100 (4)	280 ± 19 (4)	190 ± 15 (5)
Δpcst	17 ± 5 (4)	18 ± 6 (4)	9 ± 1 (2)
ΔacsΔpcst	43 ± 12 (4)	86 ± 13 (4)	21 ± 4 (2)

[a.] Activity determined by coupling synthetase-dependent AMP formation to NADH oxidation, which was detected spectrophotometrically (absorbance 365 nm). Parentheses indicates number of technical replicates.

[b.] Activity tested with 20 mM acetate, propionate, or 3-hydroxypropionate as carbon substrates.

Cell extracts of Δpcst mutant display decreased 3-hydroxypropionyl-CoA synthetase activity.

To determine if the genes deleted from the RsΔpcst171SA (Δpcst) and RsΔacsΔpcst3SA (ΔacsΔpcst) encode a CoA synthetase that has activity with 3-hydroxypropionate, a coupled enzyme assay to detect CoA synthetase activity was performed (Table 1). Cell extracts of WT, Δpcst, and ΔacsΔpcst were tested for activity with either acetate, propionate, or 3-hydroxy-propionate. It was hypothesized that Δpcst would show a greater decrease in specific activity with propionate and 3-hydroxypropionate than acetate when compared to WT due to the absence of only the annotated propionyl-CoA synthetase gene (*pcst*) in Δpcst, as opposed to other CoA synthetase genes such as acetyl-CoA synthetase. Additionally, it was hypothesized that ΔacsΔpcst would display greater decrease in synthetase activity with acetate than with propionate and 3-hydroxypropionate when compared to the specific activity of Δpcst. The CoA synthetase-specific enzyme assay results show that specific activity in Δpcst decreased for all three carbon substrates when compared to the specific activity of wild-type; an approximate 15-

fold decrease with acetate, propionate, and 3-hydroxypropionate was observed. This supports the hypothesis that Δpcst contains less CoA synthetases that have activity with acetate, propionate, and 3-hydroxypropionate in its cell extract when compared to WT. Unexpectedly, the specific activity of ΔacsΔpcst was higher than Δpcst with all three carbon substrates, which requires further study before a firm conclusion can be drawn.

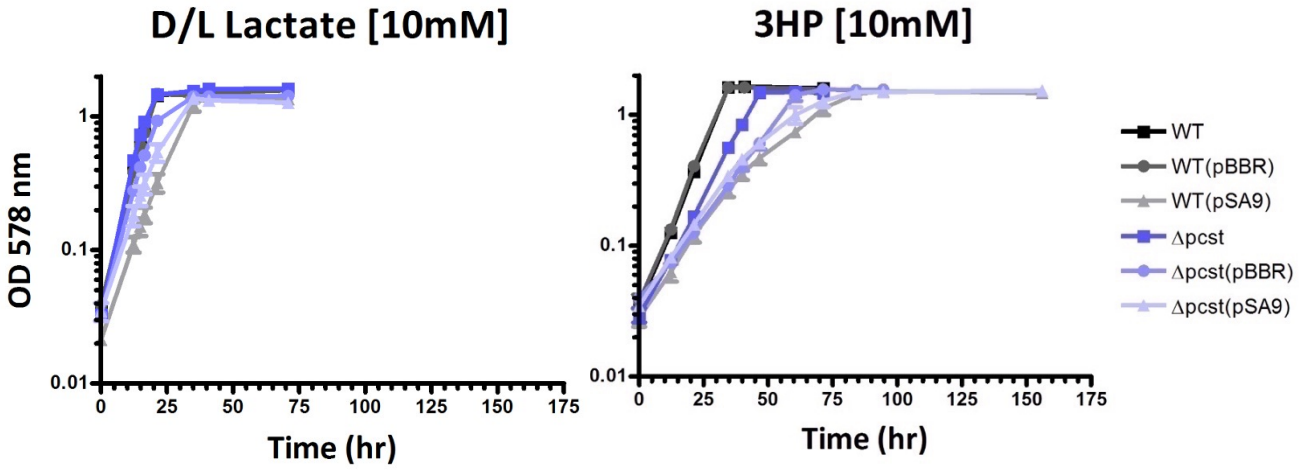

Figure 3. Photoheterotrophic growth of *R. sphaeroides* 2.4.1. *R. sphaeroides* wild-type (WT), wild-type with null vector pBBR [WT(pBBR)], wild-type complemented with *pcst* containing constitutive promoter [WT(pSA9)], Δpcst mutant, Δpcst mutant with null vector [Δpcst(pBBR)], and Δpcst mutant complemented with constitutively expressed *pcst* [Δpcst(pSA9)] were grown in minimal media containing D/L lactate (left, control) or 3-hydroxypropionate (right) as the sole carbon source. Biological triplicates of each growth experiment were performed (error bars not visible).

Table 2. Doubling time calculations based on growth experiment data from Fig. 3.

	D/L lactate	**3-hydroxypropionate**
WT	4.4 ± 0.0[a]	6.0 ± 0.1
WT(pBBR)	4.5 ± 0.2	6.1 ± 0.2
WT(pSA9)	5.9 ± 0.3	10.6 ± 0.7
Δpcst	4.5 ± 0.3	7.9 ± 0.2
Δpcst(pBBR)	5.2 ± 0.1	11.5 ± 0.6
Δpcst(pSA9)	5.7 ± 0.2	10.7 ± 0.5

[a.] Doubling time (h) ± standard deviation. All doubling time in biological triplicate.

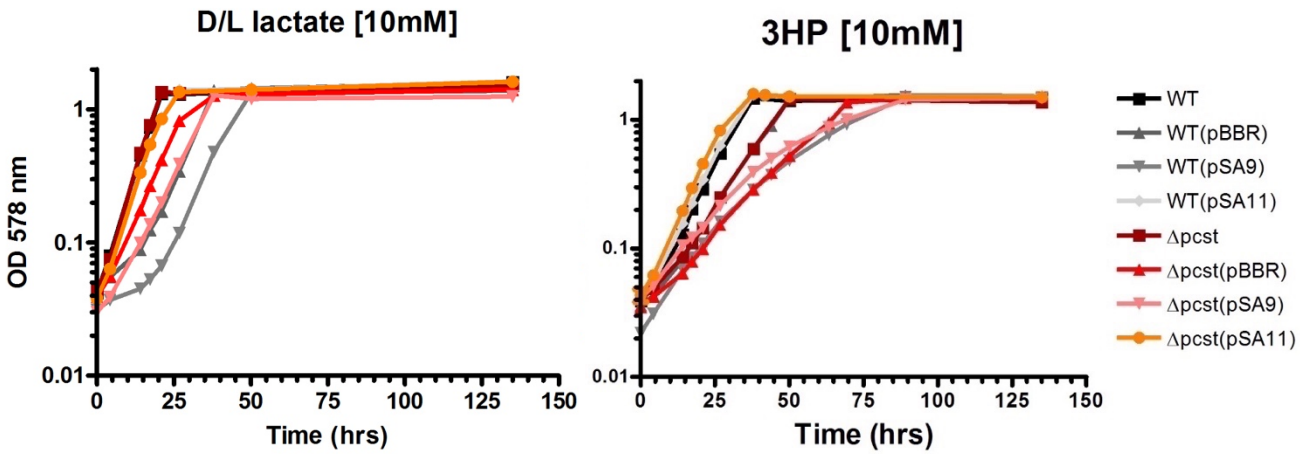

Figure 4. Photoheterotrophic growth of *R. sphaeroides* 2.4.1. *R. sphaeroides* wild-type (WT), wild-type complemented with *pcst* containing constitutive promoter [WT(pSA9)], wild-type complemented with *pcst* containing native promoter [WT(pSA11)], wild-type with null vector pBBR [WT(pBBR)], Δpcst mutant, Δpcst mutant complemented with constitutively expressed *pcst* [Δpcst(pSA9)], Δpcst mutant complemented with *pcst* containing native promoter [Δpcst(pSA11)], and Δpcst mutant with null vector [Δpcst(pBBR)] (bottom) were grown in minimal media containing D/L lactate (left, control) or 3-hydroxypropionate (right) as the sole carbon source. Biological triplicates of growth experiment with WT(pSA11) and Δpcst(pSA11) were performed (error bars not visible); for all other strains, growth experiments were performed once.

Table 3. Doubling time calculations based on growth experiment data from Fig. 4.

	D/L lactate	**3-hydroxypropionate**
WT	4.2[a]	6.8
WT(pBBR)	5.6	7.8
WT(pSA9)	6.2	10.1
WT(pSA11)	4.3 ± 0.1	6.3 ± 0.2
Δpcst	4	8.1
Δpcst(pBBR)	5.7	10.1
Δpcst(pSA9)	6.4	12.5
Δpcst(pSA11)	4.3 ± 0.1	6.1 ± 0.2

[a.] Doubling time (h) ± standard deviation for experiments performed in biological triplicate. For all other strains, growth experiments were performed once.

Expression of *pcst* from a constitutive promoter in Δpcst results in longer doubling time.

To test if growth with 3-hydroxypropionate could be restored to a doubling time similar to WT via complementation with the *pcst* gene, a growth experiment (Fig. 3, Table 2) was performed with both WT and Δpcst complemented with the *pcst* gene expressed from a constitutive promoter [WT(pSA9) and Δpcst(pSA9), respectively]. These strains were tested for growth in minimal media containing either 3-hydroxypropionate or D/L lactate; D/L lactate was a control carbon substrate because lactate is not activated by addition of CoA. It was hypothesized that complementation of Δpcst would restore the WT growth phenotype. The results, however, show an increase in doubling time for Δpcst(pSA9) (10.7 ± 0.5 h) when compared to Δpcst (7.9 ± 0.2 h) when grown with 3-hydroxypropionate. This trend was also seen with WT grown with 3-hydroxypropionate; WT(pSA9) (10.6 ± 0.7 h) displayed a higher doubling time than WT (6.0 ± 0.1 h). The increased doubling time of WT and Δpcst both complemented with constitutively expressed *pcst* gene may be associated with an overexpression of *pcst* that could negatively affect cell growth.

A growth experiment similar to that in Fig. 3 was performed with addition of WT(pSA11) and Δpcst(pSA11) complementation strains to determine the impact of constitutive *vs.* native promoter expression of *pcst* gene (Fig. 4, Table 3). Strains WT(pSA11) and Δpcst(pSA11) are complemented with *pcst* expressed from a native promoter. When grown with 3-hydroxypropionate, Δpcst(pSA11) had a doubling time similar to WT (6.1 ± 0.2 and 6.8 h, respectively), which indicates that native expression of *pcst* was able to complement Δpcst and restore cell growth to WT-like conditions. The Δpcst strain complemented with *pcst* expressed from a constitutive promoter [Δpcst(pSA9)] still displayed an increased doubling time (12.5 hr), further supporting that constitutive expression of *pcst* may be harmful to cell growth.

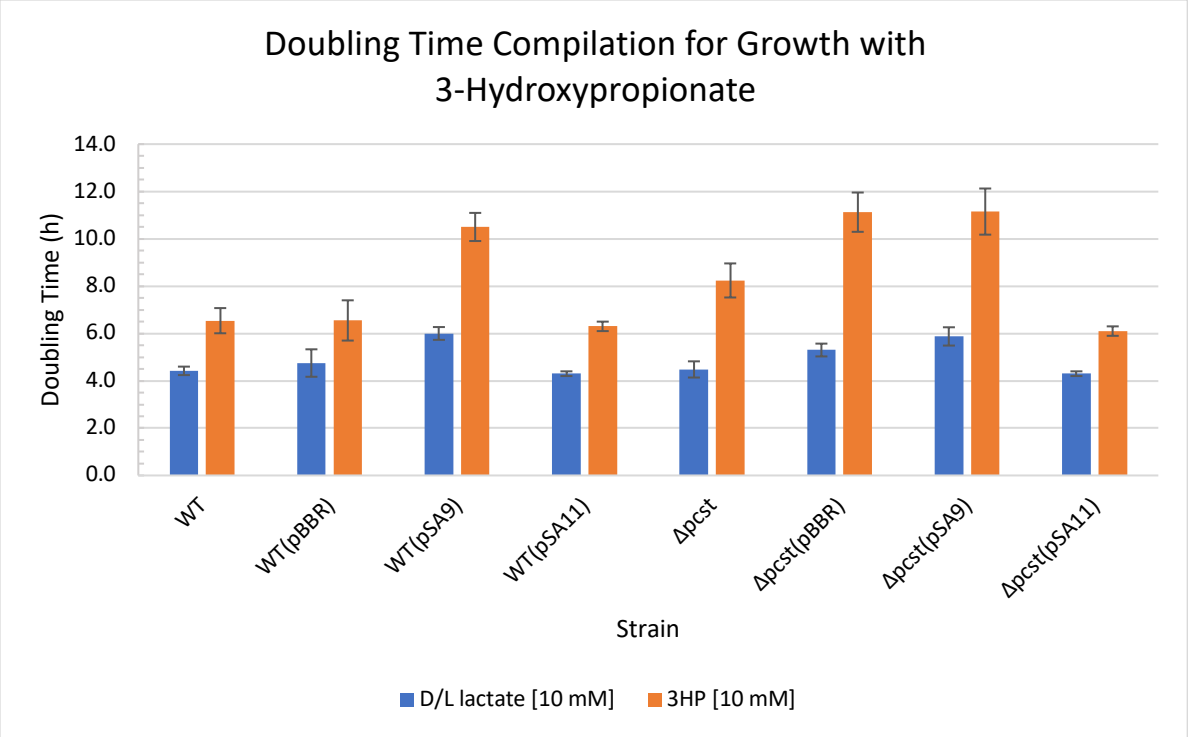

Figure 5. Compilation of doubling time calculations from growth experiments (Fig. 3,4). Additional WT and Δpcst replicates obtained from previous growth experiments under same growth conditions. Indicated strains grown with either 10 mM D/L lactate (blue, control) or 10 mM 3-hydroxypropionate (orange). Standard deviation error bars shown.

Table 4. Doubling time calculations based on Doubling Time Compilation (Fig. 5).

	D/L lactate	**3-hydroxypropionate**
WT	4.4 ± 0.2 (5)[a]	6.5 ± 0.5 (5)
WT(pBBR)	4.8 ± 0.6 (4)	6.6 ± 0.9 (4)
WT(pSA9)	6.0 ± 0.3 (4)	10.5 ± 0.6 (4)
WT(pSA11)	4.3 ± 0.1 (3)	6.3 ± 0.2 (3)
Δpcst	4.5 ± 0.3 (4)	8.2 ± 0.7 (4)
Δpcst(pBBR)	5.3 ± 0.3 (4)	11.1 ± 0.8 (4)
Δpcst(pSA9)	5.9 ± 0.4 (4)	11.2 ± 1.0 (4)
Δpcst(pSA11)	4.3 ± 0.1 (3)	6.1 ± 0.2 (3)

[a.] Mean doubling time (h) ± standard deviation (number of replicates).

Removal of *pcst* results in increased doubling time during growth with 3-hydroxy-propionate.

To test if the presence of Pcst was essential for growth with 3-hydroxypropionate, multiple growth experiments were performed comparing the growth of WT with 3-hydroxypropionate with a mutant version of WT that had the *pcst* gene removed (Δpcst) (Fig. 5, Table 4). Doubling times for WT and Δpcst with the control carbon substrate (D/L lactate) were similar (4.4 ± 0.2 h, 4.5 ± 0.3 h respectively). An increase in doubling time was observed for Δpcst when grown with 3-hydroxypropionate; WT had a doubling time of 6.5 ± 0.5 h, whereas Δpcst had a doubling time of 8.2 ± 0.7 h. The results from the strains containing the null vector (pBBR), native promoter *pcst* expression vector (pSA11), and carbon substrate (D/L lactate) controls (Fig. 5, Table 4) support that the difference in doubling time between WT and Δpcst during growth with 3-hydroxypropionate is due to the lack of *pcst* expression.

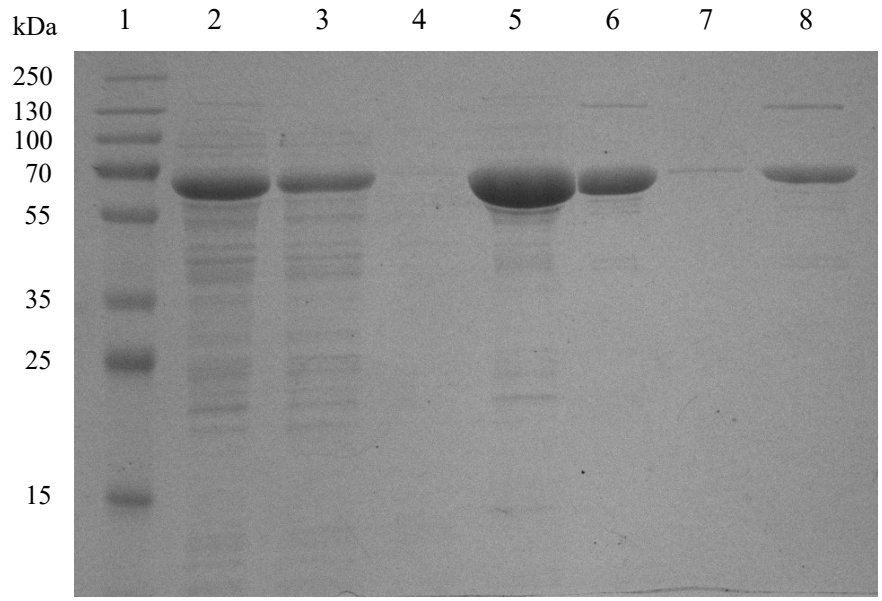

Figure 6. SDS-PAGE (10%) showing various steps of purification of His_6-tagged Pcst derived from *R. sphaeroides*. Lane 1, PageRuler Plus Prestained Protein Ladder; lane 2, cell extract protein of heterologously produced Pcst in *E. coli* (14.3 µg protein); lane 3, supernatant of cell extract precipitated with 40% ammonium sulfate (8.3 µg protein); lane 4, nickel column flow through; lane 5, 100 mM imidazole buffer fraction (18.0 µg protein); lane 6, 350 mM imidazole buffer elution fraction (5.1 µg protein); lane 7, 500 mM imidazole buffer fraction; lane 8, 350 mM imidazole buffer elution dialyzed with imidazole-free buffer (10.8 µg protein). Gel was stained with Coomassie brilliant blue.

Table 5. CoA synthetase-specific activity at various steps of His_6-tagged Pcst purification.

	Cell Extract	40% Ammonium Sulfate Fraction	100 mM Imidazole Fraction	350 mM Imidazole Fraction
Specific Activity[a] (µmol/min/mg)	24 ± 1 (2)	26 ± 3 (2)	33 (1)	38 ± 3 (2)

[a.] Activity detected by coupling synthetase-dependent AMP formation to NADH oxidation, which was detected spectrophotometrically (absorbance 365 nm). Propionate used as substrate in assay. Specific Activity ± standard deviation (number of replicates).

Immobilized Nickel Affinity Chromatography resulted in purification of His_6-Tagged Pcst.

From previous examination of cells pre- and post-induction, the size of His_6-tagged Pcst (H-Pcst) under denaturing conditions appears to be 70 kDa, which is supported by calculation of the molecular weight (72.1 kDa) based on the amino acid sequence of H-Pcst. The cell extract (Fig. 4, lane 2) and supernatant of 40% ammonium sulfate precipitation of cell extract (Fig. 6,

lane 3) contain a band at the estimated molecular weight of H-Pcst (72.1 kDa). Compared to the cell extract and precipitation fractions, the 350 mM imidazole elution fraction contained a band at the molecular weight of H-Pcst and a decrease in extraneous protein bands (Fig. 6, lane 6, dialyzed 350 mM imidazole fraction in lane 8). An increase in CoA synthetase-specific activity from cell extract (24 ± 1 μmol/min/mg) to 350 mM imidazole fraction (38 ± 3 μmol/min/mg) (Table 5) is observed; the marginal increase in specific activity suggests that a high ratio of Pcst to total protein was already present in cell extract prior to Nickel-NTA column purification. The dialyzed 350 mM imidazole elution fraction was used in subsequent assays to determine substrate-dependent H-Pcst activity.

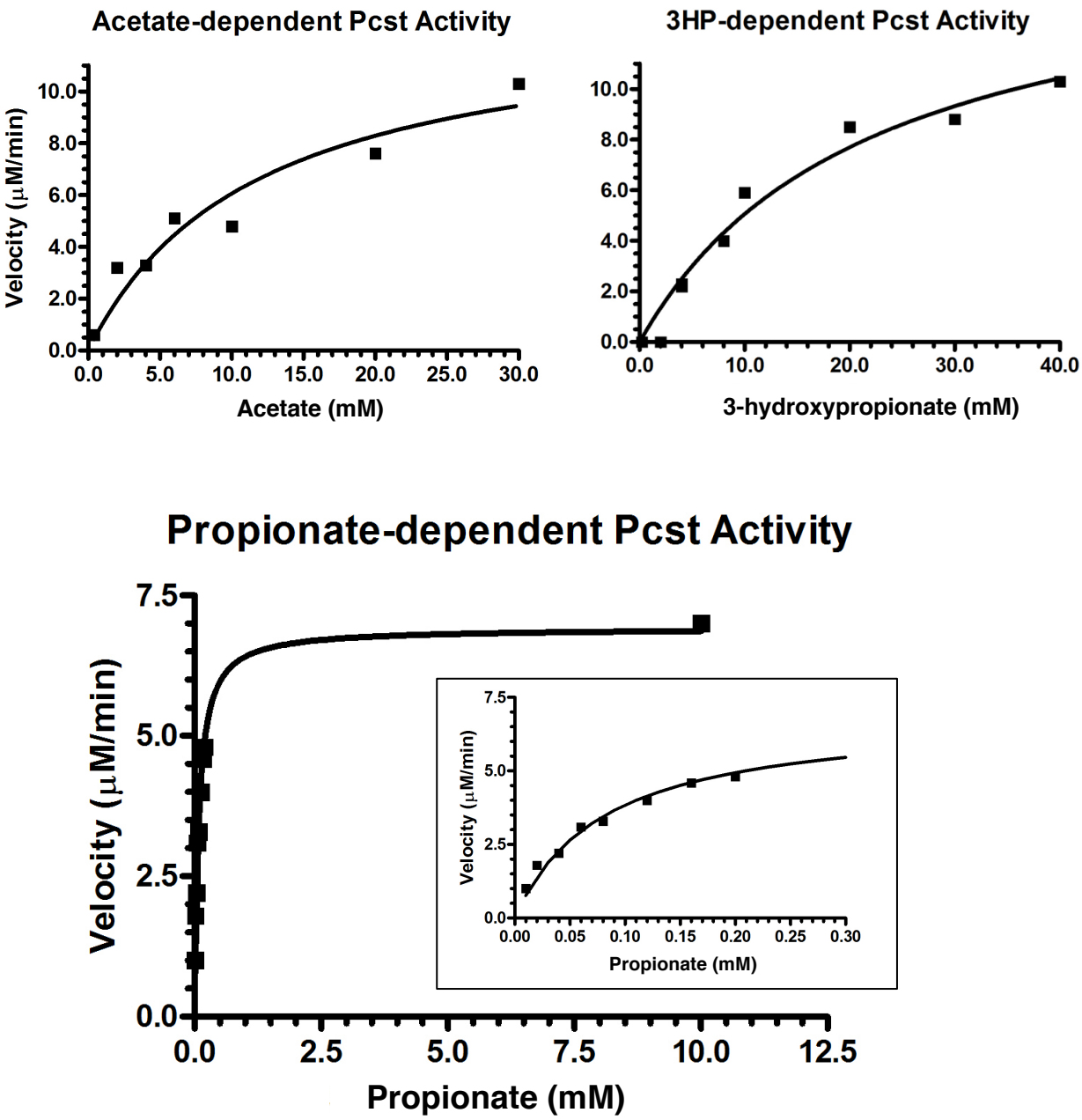

Figure 7. Michalis-Menten plots of Pcst activity with various limiting concentrations of acetate (top left), 3-hydroxypropionate (top right), and propionate (bottom). Velocity of reaction was calculated, plotted, and fit to the Michalis-Menten equation ($V_0 = V_{max}\frac{[S]}{[S]+K_m}$) to calculate K_m and v_{max} values for a single trial.

Table 6. Kinetic parameters for purified His_6-tagged Pcst activity with acetate, propionate, and 3-hydroxypropionate.

	Acetate	**Propionate**	**3-hydroxypropionate**
K_m **(mM)**	12 ± 5[a]	0.080 ± 0.007	22 ± 6
V_{max} **(µM/min)**	13 ± 2	6.9 ± 0.2	16 ± 2
k_{cat} **(s^{-1})**	2.9	3.9	1.8
k_{cat}/K_m **(mM^{-1} s^{-1})**	0.25	48	0.082

[a.] Pcst activity determined by coupling Pcst-dependent AMP formation to NADH oxidation, which was detected spectrophotometrically (absorbance 365 nm). Standard deviations calculated from fit of data to the Michalis-Menten equation.

Pcst displays high catalytic efficiency with propionate.

Substrate-dependent coupled kinetic assays were performed to determine the kinetic parameters of His_6-tagged Pcst (H-Pcst) and activity with acetate, propionate, and 3-hydroxy-propionate (Fig. 7, Table 6). It was hypothesized that H-Pcst would have a lower K_m value and higher catalytic efficiency with propionate than acetate since Pcst was initially annotated as a propionyl-CoA synthetase due to its homology to other propionyl-CoA synthetases. Additionally, H-Pcst was expected to have a similar K_m and catalytic efficiency with 3-hydroxy-propionate as propionate due to the decrease in CoA synthetase-specific activity of Δpcst cell extracts with substrates acetate and 3-hydroxypropionate (Table 1). Substrate-dependent enzyme assay results show a high specificity for propionate to H-Pcst (K_m value of 0.080 ± 0.007 mM), whereas H-Pcst displays a much lower specificity with acetate and 3-hydroxypropionate (12 ± 5 and 22 ± 6 mM, respectively). Results also show that H-Pcst has a higher catalytic efficiency (k_{cat}/K_m) with propionate (48 mM^{-1} s^{-1}) than acetate (0.25 mM^{-1} s^{-1}) or 3-hydroxypropionate (0.082 mM^{-1} s^{-1}). The difference in both K_m and catalytic efficiency values between propionate and acetate/3-hydroxypropionate is greater than two orders of magnitude, suggesting a significantly higher specificity and activity of Pcst with propionate when compared to acetate and 3-hydroxypropionate.

Discussion

Pcst partially contributes to 3-hydroxypropionate assimilation.

Growth analysis of *pcst* mutants allows insight into the use of 3-hydroxypropionate *in vivo*. An increase in doubling time for *R. sphaeroides* lacking *pcst* observed in growth with 3-hydroxypropionate indicates that Pcst plays a role in 3-hydroxypropionate assimilation and the absence of Pcst has negative impacts on cellular growth. However, only a change in doubling time from 6.5 to 8.2 hours was observed during growth with 3-hydroxypropionate with the strain lacking *pcst*, which suggests that this enzyme is not the sole or predominant contributor to 3-hydroxypropionate assimilation. This claim is supported by substrate-specific Pcst kinetics data; a 100-fold reduction in catalytic efficiency of H-Pcst with 3-hydroxypropionate in comparison to propionate was observed. Because Pcst does not have high catalytic efficiency with 3-hydroxy-propionate, it is unlikely that this enzyme is the sole contributor to 3-hydroxypropionate activation.

Because Pcst only partially contributes to 3-hydroxypropionate assimilation, it is likely that 3-hydroxypropionate activation is predominantly catalyzed by a different enzyme. A possible enzyme candidate is succinyl-CoA:3-hydroxypropionate CoA transferase, which could transfer the CoA from succinyl-CoA to 3-hydroxypropionate. This would permit the recycling of CoA during conversion of succinyl-CoA to succinate in the citric acid cycle[5]. Since synthetase activity is still detected in *R. sphaeroides* strains lacking both *acs* and *pcst*, it is also possible that an unidentified synthetase is activating 3-hydroxypropionate.

Gene *pcst* encodes a propionyl-CoA synthetase.

Based on the results from enzymatic activity of cell extracts and purified protein, Pcst can be characterized in its function and efficiency with various carbon substrates. The decreased in CoA synthetase activity in strains lacking *pcst* indicate that *pcst* encodes a synthetase with the ability to add CoA to acetate, propionate, and 3-hydroxypropionate. Further support for the CoA synthetase activity of Pcst comes from an increase in CoA synthetase-specific activity during the purification of Pcst (Table 5). This enzyme appears to be promiscuous due to observed decrease in CoA synthetase activity with acetate, propionate, and 3-hydroxypropionate in strains lacking *pcst*. The ability of Pcst to add CoA to the carbon substrates tested indicates that this enzyme may play a role in the activation and assimilation of compounds such as propionate, acetate, and 3-hydroxypropionate *in vivo*.

However, Pcst has high efficiency with propionate as displayed by the 100-fold greater catalytic efficiency of purified H-Pcst with propionate over acetate or 3-hydroxypropionate. The ability of Pcst to add CoA to propionate indicates that this enzyme predominately plays a role in propionate activation and assimilation; additionally, Pcst may have a minor contribution in assimilation of similar compounds such as acetate and 3-hydroxypropionate *in vivo*. Interestingly, it appears that Pcst is able to differentiate and discriminate between compounds that differ only slightly in carbon number or functional group. Further examination of activity of Pcst with other compounds, such as butyrate, and structural analysis of the enzyme would allow firmer conclusions with respect to its substrate specificity.

Regulation of *pcst* expression may impact cellular growth.

The inability of *pcst* expression from a constitutive promoter to complement Δpcst was an unexpected observation. Furthermore, constitutive *pcst* expression in WT also resulted in a longer doubling time. The observation of increased doubling time when both WT and Δpcst had constitutive expression of *pcst* suggests that cell growth is hindered by higher expression of *pcst*. Moving forward, detecting the difference in CoA synthetase-specific activity between *R. sphaeroides* WT, Δpcst(pSA9), WT(pSA9), and Δpcst(pSA11) would aid in understanding how regulation of *pcst* impacts cellular growth. The mechanism behind this observation is unclear, but possible explanations include formation of CoA synthetase byproducts that are detrimental to the cell in elevated quantities or limiting the availability of free CoA for other critical metabolic processes.

References

1. Kumar, V. & Ashok, S. Recent advances in biological production of 3-hydroxypropionic acid. *Biotechnol. Adv.* **31**, 945–961 (2013).
2. Meng, D.-C. *et al.* Production of poly(3-hydroxypropionate) and poly(3-hydroxybutyrate-co-3-hydroxypropionate) from glucose by engineering *Escherichia coli*. *Metab. Eng.* **29**, 189–195 (2015).
3. Fuchs, G. & Berg, I. A. Unfamiliar metabolic links in the central carbon metabolism. *J. Biotechnol.* **192**, 314–322 (2014).
4. Schneider, K., Asao, M., Carter, M. S. & Alber, B. E. *Rhodobacter sphaeroides* uses a reductive route via propionyl coenzyme A to assimilate 3-hydroxypropionate. *J. Bacteriol.* **194**, 225–32 (2012).
5. Mullins, E. A., Francois, J. A. & Kappock, T. J. A specialized citric acid cycle requiring succinyl-coenzyme A (CoA):acetate CoA-transferase (AarC) confers acetic acid resistance on the acidophile *Acetobacter aceti*. *J. Bacteriol.* **190**, 4933–40 (2008).
6. Veit, A. *et al.* Pathway identification combining metabolic flux and functional genomics analyses: acetate and propionate activation by *Corynebacterium glutamicum*. *J. Biotechnol.* **140**, 75–83 (2009).
7. Horswill, A. R. & Escalante-Semerena, J. C. Characterization of the propionyl-CoA synthetase (PrpE) enzyme of *Salmonella enterica*: residue Lys592 is required for propionyl-AMP synthesis. (2002).
8. Li, R. *et al.* Purification and characterization of the acetyl-CoA synthetase from *Mycobacterium tuberculosis*. *Acta Biochim. Biophys. Sin. (Shanghai).* **43**, 891–899 (2011).
9. Alber, B. E., Spanheimer, R., Ebenau-Jehle, C. & Fuchs, G. Study of an alternate

glyoxylate cycle for acetate assimilation by *Rhodobacter sphaeroides*. *Mol. Microbiol.* **61**, 297–309 (2006).

10. Hanahan, D. Studies on transformation of *Escherichia coli* with plasmids. *J. Mol. Biol.* (1983).

11. Simon, R., Priefer, U. & Pühler, A. A broad host range mobilization system for *in vivo* genetic engineering: transposon mutagenesis in gram negative bacteria. *Bio/Technology* **1**, 784–791 (1983).

12. Hockney, R. C. Recent developments in heterologous protein production in *Escherichia coli*. *Trends Biotechnol.* **12**, 456–463 (1994).

13. Schäfer, A. *et al.* Small mobilizable multi-purpose cloning vectors derived from the *Escherichia coli* plasmids pK18 and pK19: selection of defined deletions in the chromosome of *Corynebacterium glutamicum*. *Gene* **145**, 69–73 (1994).

14. Kovach, M. E., Phillips, R. W., Elzer, P. H., Roop, R. M. & Peterson, K. M. pBBR1MCS: a broad-host-range cloning vector. *Biotechniques* **16**, 800–2 (1994).

Acknowledgement

Funding for this research was supported by the National Science Foundation. Thank you to the Tabita Laboratory and Dr. Justin North for use and assistance with the French press, Rappleye Laboratory for use of camera and imaging software, Dr. Eric Danhart for assistance in protein quantification, and Dr. Marie Asao for her previous work that supported this study. Thank you to Dr. Birgit Alber for her essential guidance and advice in formulation of this research project, Lexie Kuzmishin Nagy and Suzy Bangudi for keeping me sane in the laboratory, and Steven Carlson for his support, mentorship, and immense time spent putting up with me.

Appendix

Table 7. Strains utilized in work.

Name	Relevance	Reference
Escherichia coli DH5α[10]	Cloning strain	Hanahan (1983)
Escherichia coli S17-1[11]	Donor strain for conjugation (kanamycin resistant)	Simon *et* al. (1983)
Escherichia coli SM10[11]	Donor strain for conjugation (streptomycin resistant)	Simon *et* al. (1983)
Escherichia coli BL21[12]	Strain for heterologous protein production (ampicillin resistant)	Hockney (1994)
Rhodobacter sphaeroides 2.4.1	Wild type	DSMZ 158
WT(pSA8)	WT plus plasmid pSA8 (expression of *acs* with constitutive promoter)	This work
WT(pSA9)	WT plus plasmid pSA9 (expression of *pcst* with constitutive promoter)	This work
WT(pSA10)	WT plus plasmid pSA10 (expression of *acs* with native promoter)	This work
WT(pSA11)	WT plus plasmid pSA11 (expression of *pcst* with native promoter)	This work
WT(pBBR)	WT plus plasmid pBBR (empty vector)	This work
RsΔacs21SA	In-frame deletion of *acs*	This work
RsΔacs21SA(pSA8)	In-frame deletion of *acs* plus plasmid pSA8 (expression of *acs* with constitutive promoter)	This work
RsΔacs21SA(pSA10)	In-frame deletion of *acs* plus plasmid pSA10 (expression of *acs* with native promoter)	This work
RsΔpcst17SA	In-frame deletion of *pcst*	This work
RsΔpcst17SA(pBBR)	In-frame deletion of *pcst* plus plasmid pBBR (empty vector)	This work
RsΔpcst17SA(pSA9)	In-frame deletion of *pcst* plus plasmid pSA9 (expression of *pcst* with constitutive promoter)	This work
RsΔpcst17SA(pSA11)	In-frame deletion of *pcst* plus plasmid pSA11 (expression of *pcst* with native promoter)	This work
RsΔacsΔpcst3SA	In-frame deletion of *acs* and *pcst*	This work

Table 8. Plasmids utilized in this work.

Name	Relevance	Reference
pK18mobsacB[13]	Conjugation plasmid containing *sacB* for selection with sucrose	Schafer et al. (1994)
pUC19[13]	Cloning vector	Schafer et al. (1994)
pET16b	Expression plasmid containing IPTG-inducible system	Novagen
pSC114	Inactivation construct for *acs* (*rsp_0579*)	Steven Carlson
pSC115	Inactivation construct for *pcst* (*rsp_1592*)	Steven Carlson
pMA24-4	Expression plasmid for His-Acs (pET16b-derived)	Marie Asao
pMA18-4	*pcst* inserted into pUC19; intermediate for pMA27-1	Marie Asao
pMA26-1	*pcst* inserted into pUC19; intermediate for pMA27-1	Marie Asao
pMA27-1	Expression plasmid for His-Pcst (pET16b-derived)	Marie Asao
pBBR[14]	"Empty vector"	Kovach *et* al. (1994)
pSC75	Derived from pBBR, addition of rrnB promoter	Steven Carlson
pSA8	Complementation construct for *acs* (rrnB promoter)	This work
pSA9	Complementation construct for pcst (rrnB promoter,)	This work
pSA10	Complementation construct for *acs* (native promoter)	This work
pSA11	Complementation construct for *pcst* (native promoter)	This work

Table 9. Primers utilized in this work.

Primer	DNA sequence (5'-3')	Use
dASynUp_F	CCGGTTCTTGCGGTTGGCGATCAGCACGGATGCAGCATAC	*acs* inactivation
dASynUp_R	TTGC*AAGCTT*CCTGCTCGTGGTGTTC	*acs* inactivation, Δ*acs* sequencing
dASynDn_F	CCATTGGACTTCCTCCC*TCTAGA*TTTCTTC	*acs* inactivation
dASynDn_R	CTGATCGCCAACCGCAAGAACC	*acs* inactivation
dASyn_1xo_UpR	CGCCATCGAGTCGCTTCTTTC	Δ*acs* sequencing
dASyn_1xo_DnF	GCACGAGGAAGACGTAGATGGAG	Δ*acs* sequencing
RSP579_R	GGGCTGCTTGAAGCTTTCGTGGTATCCC	Δ*acs* sequencing
dPSynUp_F	GGGCATCTTGAACTCCTGCCCGTCGGGATCCTCCAGAGACCATTTGTAG	*pcst* inactivation
dPSynUp_R	GCTATCGCG*AAGCTT*GGGAGAGCTACCAC	*pcst* inactivation
dPSynDn_F	AGCACCGAGC*TCTAGA*CCATCTG	*pcst* inactivation
dPSynDn_R	GACGGGCAGGAGTTCAAGATG	*pcst* inactivation
CoAligase_F	CGCTTCAGCCAAAGGTTGTGCATTTC	Δp*cst* sequencing
dPSynUp_F	GGGCATCTTGAACTCCTGCCCGTCGGGATCCTCCAGAGACCATTTGTAG	Δp*cst* sequencing
dPSynDn_F	AGCACCGAGCTCTAGACCATCTG	Δp*cst* sequencing
dPSyn_1xo_UpR	ATCCCGGCGGATCGTCTTTG	Δp*cst* sequencing
dPSyn_1xo_DnF	ACCGCCTTGTTGATCGAACC	Δp*cst* sequencing
dASyn_1xo_UpF	CGCCCGACGAAAGCTGGAC	genotype Δ*acs*
dASyn_1xo_UpR	CGCCATCGAGTCGCTTCTTTC	genotype Δ*acs*
dASyn_1xo_DnF	GCACGAGGAAGACGTAGATGGAG	genotype Δ*acs*
dASyn_1xo_DnR	GATGCGTTACACTCTGGCTAATGG	genotype Δ*acs*
dPSyn_1xo_UpF	CGCTTCAGCCAAAGGTTGTG	genotype Δ*pcst*
dPSyn_1xo_UpR	ATCCCGGCGGATCGTCTTTG	genotype Δ*pcst*
dPSyn_1xo_DnF	ACCGCCTTGTTGATCGAACC	genotype Δ*pcst*
dPSyn_1xo_DnR	CCGCAGAGGCTCCAACTTAAC	genotype Δ*pcst*
RSP579_F5	CTC ATA TGT TAC ACT CTG GCT AAT GG	Acs expression
RSP579_R	GGG CTG CTT GAA GCT TTC GTG GTA TCC C	Acs expression
RSP579exp_NdeIF	TGG AGG AGC TCA TAT GGA TCA CGC TCA GG	Acs expression
RSP579exp_HindIIIR	CAG CAC AAG CTT ACG GGT GGT CGT CTC	Acs expression
RSP1592_F4	TGG CCG CAG AGG CTC CAT ATG AAC GTG	Pcst expression
RSP1592_R	CGC TTC AGC CAA AGC TTG TGC ATT TCC	Pcst expression
RSP1592exp_NdeIF	TTA ACA GCA TAT GCG CGC CGA GGG AGG	Pcst expression
RSP1592exp_HindIII	GGG CTC GAA GCT TGA TGC GCG ACC GTG	Pcst expression

Primer	DNA sequence (5'-3')	Use
acs_speI_R	ATAGGCGTATCACTAGTCCCTTTCGTCTTC	Δ*acs,* Δ*pcst* constitutive complementation
acs_ndeI_F	AAGGTCGTCATATGGATCAC	Δ*acs* constitutive complementation
RSP_1592_ndeI_F	CCATATCGAAGGTCGTCATATGC	Δ*pcst* constitutive complementation
acs_sacI_F	ACATTGAGCTCGCAGACGCGATCCTTTC	Δ*acs* native complementation
COMPacs_speI_R	GCGGACTAGTTGAAGCTGTCGTGGTATC	Δ*acs* native complementation
pcst_sacI_F	TGAGCTCCCTCGCCCATATCGTAACCG	Δ*pcst* native complementation
COMPpcst_speI_R	CCGGACTAGTTCGCAGGGCTCGCCTCTTG	Δ*pcst* native complementation